Chemistry of Metals and Alloys

Chem. Met. Alloys 7 (2014) 42-55
Ivan Franko National University of Lviv
www.chemetal-journal.org

New ternary phases from the *R*–Au–Ga systems (*R* = Gd-Tm)

Yuriy VERBOVYTSKYY[1,2]*

[1] *Department No. 27, Karpenko Physico-Mechanical Institute, National Academy of Sciences of Ukraine, Naukova St. 5, 79060 Lviv, Ukraine*
[2] *Campus Tecnológico e Nuclear, Instituto Superior Técnico, Universidade Técnica de Lisboa/CFMC–UL, Estrada Nacional 10, 2695-066 Bobadela LRS, Portugal*
* *Corresponding author. E-mail: yuryvv@bigmir.net*

Dedicated to Evgen I. Gladyshevskii (1924-2012)

Received December 2, 2013; accepted June 26, 2014; available on-line November 10, 2014

Twenty rare-earth gold gallides, RAu_3Ga_7 ($ScRh_3Si_7$-type, space group *R*-3*c*, *Z* = 6, *hR*66), $RAu_{3\pm x}Ga_{3\pm x}$ (YCd_6-type, space group *Im*-3, *Z* = 24, *cI*68), $RAu_{1+x}Ga_{2-x}$ ($MgCuAl_2$-type, space group *Cmcm*, *Z* = 4, *oS*16) (*R* = Gd-Tm) and $R_{14}Au_{34+x}Ga_{17-x}$ ($Gd_{14}Ag_{51}$-type, space group *P*6/*m*, *Z* = 1, *hP*65) (*R* = Er, Tm), were synthesized by arc-melting, followed by annealing at 400-600°C. Six phases $RAu_{1+x}Ga_{3-x}$ ($BaAl_4$-type, space group *I*4/*mmm*, *Z* = 2, *tI*10) (*R* = Gd) and $R_3Au_{3+x}Ga_{8-x}$ (La_3Al_{11}-type, space group *Immm*, *Z* = 2, *oI*26) (*R* = Tb-Tm) were prepared by the flux method. Their crystal structures were studied by X-ray powder or single crystal diffraction. Structural peculiarities, coordination and interaction of the atoms in the investigated compounds are briefly discussed.

Rare-earth intermetallics / Ternary gallides / Crystal growth / Single crystal / X-ray diffraction / Crystal structure

Introduction

Ternary intermetallic compounds $R_xM_yX_z$ (*R* = rare-earth element, *M* = *d*-metal, *X* = *p*-metal) have been intensively studied over the last 40 years with respect to phase analysis, crystal structures, and physical properties. For most families of compounds, *e.g.* borides, gallides, indides, *etc.*, various books and extensive review articles have been published [1-8]. Among the many ternary *R*–*M*–*X* systems, those with the noble metals have so far been poorly investigated [9]. Results on the identification of new *R*–Au–Al compounds have already been presented in a previous work [10]. Eight new rare-earth gold aluminides, $R_3Au_xAl_{11-x}$ (*R* = Y, Gd, Ho, Er, and Tm), $RAuAl_3$ (*R* = Yb and Gd) and RAu_3Al_7 (*R* = Y), have been synthesized and their crystal structures solved from powder X-ray diffraction data. This paper presents a further contribution to the study of ternary rare-earth – gold – gallium systems.

Systematic investigations of ternary *R*–Au–Ga systems have only been performed for ytterbium. The isothermal section of the Yb–Au–Ga system was built at 600°C [11], and ten ternary phases were reported [11-19]: $YbAu_3Ga_7$ ($ScRh_3Si_7$-type), $YbAu_{2.90\text{-}4.41}Ga_{3.10\text{-}1.59}$ (own type), $YbAu_{0.15}Ga_{3.85}$ ($CaAu_{0.15}Ga_{3.85}$-type), $YbAu_{0.2\text{-}1.5}Ga_{3.8\text{-}2.5}$ ($BaAl_4$-type), $Yb_3Au_{4.8}Ga_{6.2}$ (La_3Al_{11}-type), $Yb_3Au_{5.5}Ga_{5.5}$ (own type), $Yb_{14}Au_{32.5\text{-}40.2}Ga_{18.5\text{-}10.8}$ ($Gd_{14}Ag_{51}$-type), $YbAu_{0.26\text{-}0.92}Ga_{1.74\text{-}1.08}$ ($CeCu_2$-type), $YbAu_{0.94\text{-}1.17}Ga_{1.06\text{-}0.83}$ (TiNiSi-type), and $YbAu_{1.21\text{-}1.31}Ga_{0.79\text{-}0.69}$ ($CeCu_2$-type). Investigations on alloys from the RAu_2–RGa_2 (*R* = Y, La, Ce, Pr, Nd, Sm, Eu, Gd, Tb, Dy, Ho, Er, Tm, Yb, Lu) cross-section were performed in [17-20]. Structural and magnetic studies of RAu_xGa_{4-x} ($BaAl_4$-type) (*R* = La, Ce, Pr, Nd, Sm, Gd, Yb) and $R_3Au_xGa_{11-x}$ (La_3Al_{11}-type) (*R* = Y, Gd, Tb, Dy, Ho, Er, Tm, Yb) phases can be found in [12,14,21-24]. Moreover, formation of the $LuAu_{1.25}Ga_{1.75}$ ($MgCuAl_2$-type) and $EuAu_{1.86}Ga_{5.14}$ ($SrAu_2Ga_5$-type) compounds was reported in [25,26].

Experimental details

Starting materials for the synthesis of the *R*–Au–Ga alloys were rare-earth ingots (*R* > 99.9 wt.%), gold plate (99.99 wt.%) and gallium pieces (99.999 wt.%). Samples with a total weight of 300 mg were prepared by arc-melting buttons in a water-cooled copper crucible with a tungsten electrode under a purified argon atmosphere, using Ti/Zr as a getter. The products were turned over and re-melted at least three times in order to ensure homogeneity. Fragments of

the ingots were wrapped in tantalum foil and sealed in evacuated quartz tubes. Annealing was performed at 400-600ºC for one month. After that, the samples were quenched by submerging the quartz tubes in cold water.

Single crystals were grown by the self-flux method. Rare-earth metals, gold and gallium were placed into an alumina crucible in a 1:2:8 or 1:2:6 ratio. The crucibles were inserted into quartz tubes, which were evacuated, sealed, heated at 1000ºC for 1 h and cooled down to 400ºC within 3 days. Block-like crystals of up to 3 mm^3 size were mechanically isolated and cleaned with a hot concentrated aqueous solution of potassium hydroxide and a solution of iodine in dimethylformamide. No noticeable degradation of the crystals in air was observed.

The products were crushed, powdered in an agate mortar, and examined by X-ray powder diffraction. Phase analysis of the alloys was carried out on X-ray diffraction patterns obtained on HZG-4a and DRON3 diffractometers (Cu $K\alpha$ radiation). X-ray structural studies were performed using a PANalytical X'Pert Pro diffractometer (Cu $K\alpha$ radiation). The scans were taken in the $\theta/2\theta$ mode with the following parameters: 2θ region 15-120º; step scan 0.03º; counting time per step 20-30 s. The theoretical powder patterns were calculated with the help of the PowderCell program [27]. The lattice parameters were obtained by least-squares fitting using the Latcon program [28]. The FullProf [29] program was used for the Rietveld refinements. A pseudo-Voigt profile shape function was used. The background was refined with a polynomial function.

Suitable silver-colored fragments of the crystals were mounted onto the goniometer of a CAD4 diffractometer equipped with graphite monochromatized Mo $K\alpha$-radiation and a scintillation counter with pulse height discrimination. Scans were taken in the $\omega/2\theta$ mode. Empirical absorption corrections were applied on the basis of ψ-scan data. The crystal structures were refined using SHELXL-97 [30] (full-matrix least-squares on F^2). The unit cell parameters were obtained by least-squares refinement of the 2θ values of 25 intense and well-centered reflections from various parts of the reciprocal space ($15º < 2\theta < 35º$).

The microstructure of the selected samples was studied on polished and etched surfaces, by using an optical microscope Olympus OM150, or observed by electron microscopy, by using an EVO 40XVP scanning electron microscope (SEM), complemented with energy dispersive X-ray spectroscopy (EDS).

Results and discussion

The new RAu$_{3\pm x}$Ga$_{3\pm x}$ (YCd_6 structure type), RAu$_{1+x}$Ga$_{2-x}$ ($MgCuAl_2$ structure type) (R = Gd-Tm) and R_{14}Au$_{34+x}$Ga$_{17-x}$ ($Gd_{14}Ag_{51}$ structure type) (R = Er, Tm) phases were observed in as-cast samples as well as in alloys annealed at 500-600ºC, while the RAu$_3$Ga$_7$ ($ScRh_3Si_7$ structure type) (Gd-Tm) compounds were identified in alloys annealed at 400ºC. Their crystal structures were studied by means of powder X-ray diffraction.

The ground aggregates of the single crystals were also characterized by powder X-ray diffraction. The formation of the earlier reported RAu$_{1+x}$Ga$_{3-x}$ ($BaAl_4$ structure type) (R = Gd) and R_3Au$_{3+x}$Ga$_{8-x}$ (La_3Al_{11} structure type) (R = Tb-Tm) phases was confirmed. The crystal structures of these phases were refined for the first time.

The results of Rietveld refinement for selected *R*–Au–Ga alloys are shown in Fig. 1. Refined lattice parameters are summarized in Table 1. Atomic coordinates, thermal parameters, and interatomic distances for the atoms of the *R*–Au–Ga compounds can be found in Table 2 (R = Tm) and Table S1 (R = Gd-Er) and Table S2 (R = Gd-Tm) (Supplementary data).

Single crystal X-ray diffraction studies were also performed for the GdAu$_{1+x}$Ga$_{3-x}$, Dy$_3$Au$_{3+x}$Ga$_{8-x}$ and Er$_3$Au$_{3+x}$Ga$_{8-x}$ phases. Details of the data collection and structure refinements are presented in Table 3. The final atom coordinates and displacement parameters are given in Tables 4-6.

A brief discussion of the crystal structures of the RAu$_3$Ga$_7$, RAu$_{3\pm x}$Ga$_{3\pm x}$, R_{14}Au$_{34+x}$Ga$_{17-x}$, RAu$_{1+x}$Ga$_{2-x}$, and R_3Au$_{3+x}$Ga$_{8-x}$ ternary phases is given below.

RAu$_3$Ga$_7$ phases

The new RAu$_3$Ga$_7$ intermetallic compounds belong to the rhombohedral structure type $ScRh_3Si_7$ (space group $R\bar{3}c$, Z = 6, $hR66$). Here, the rare-earth atoms occupy the Sc (6*b*) site; Au atoms are located in the Rh (18*e*) positions, and Ga atoms are situated in the positions of Si (6*a* and 18*f*). Unit cell and complex three-dimensional [Au$_3$Ga$_7$] networks are shown in Fig. 2*a*. The Au–Ga distances within this network extend between 2.584 and 2.594 Å (Au–Ga1), and 2.562 and 2.680 Å (Au–Ga2), being considerably shorter than the sum (2.83 Å) of the radii of the respective elements (Au+Ga) [31]. The shorter Ga–Ga contacts (2.755-2.785 Å) are in good agreement with the sum of atomic radii of Ga (2.78 Å). The *R*–Au and *R*–Ga distances (3.255-3.274 Å and 3.241-3.265 Å) are somewhat longer than the sums of $r_R + r_{Au}$ and $r_R + r_{Ga}$ [31], respectively.

The *R* atoms are located inside 18-vertex pseudo Frank-Kasper polyhedra. The coordination polyhedra of the Au atoms are tri-capped deformed trigonal prisms. The neighbors of the Ga1 atoms form equatorially tri-capped deformed trigonal prisms. 10-vertex polyhedra (defected icosahedra) are the coordination spheres of the Ga2 atoms.

From a commonly used geometrical point of view (Fig. 2*b*), in the structure of RAu$_3$Ga$_7$ compounds the Au atoms form a hexagonal closed-packed arrangement. The Ga atoms form tetrahedra connected by common vertices to [Ga$_7$] clusters. Two thirds of

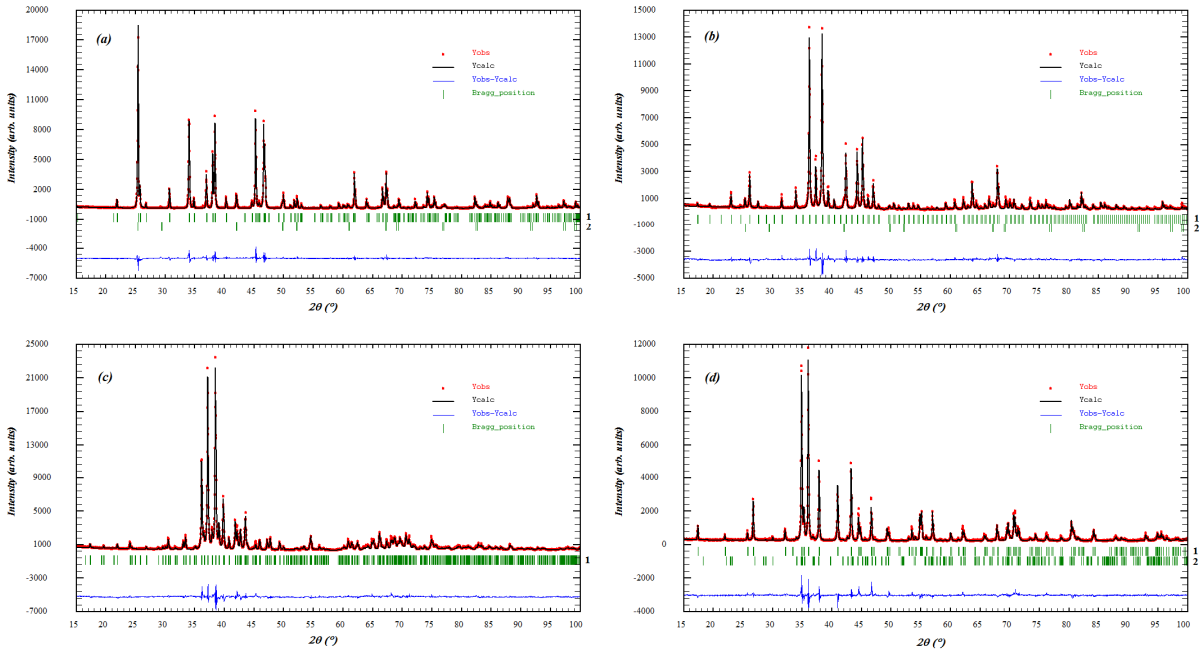

Fig. 1 Rietveld refinement of the samples (*a*) $Er_9Au_{27}Ga_{45}$ (1 – $ErAu_3Ga_7$, 2 – $AuGa_2$); (*b*) $Dy_{14}Au_{43}Ga_{43}$ (1 – $DyAu_{3\pm x}Ga_{3\pm x}$, 2 – $AuGa_2$); (*c*) $Er_{22}Au_{49}Ga_{29}$ (1 – $Er_{14}Au_{34}Ga_{17}$); (*d*) $Tm_{25}Au_{30}Ga_{45}$ (1 – $TmAuGa_2$, 2 – $Tm_3Au_3Ga_8$).

Table 1 Crystallographic data of the ternary *R*–Au–Ga phases.

Phase	Structure type	Lattice parameters			
		a (Å)	*b* (Å)	*c* (Å)	*V* (Å^3)
$GdAu_3Ga_7$	$ScRh_3Si_7$	8.13960(6)	–	20.8023(2)	1193.571(17)
$TbAu_3Ga_7$	$ScRh_3Si_7$	8.13096(7)	–	20.7785(3)	1189.67(2)
$DyAu_3Ga_7$	$ScRh_3Si_7$	8.12489(9)	–	20.7576(3)	1186.71(3)
$HoAu_3Ga_7$	$ScRh_3Si_7$	8.12063(10)	–	20.7408(3)	1184.50(3)
$ErAu_3Ga_7$	$ScRh_3Si_7$	8.11555(10)	–	20.7238(3)	1182.05(3)
$TmAu_3Ga_7$	$ScRh_3Si_7$	8.10986(10)	–	20.7073(4)	1179.45(3)
$GdAu_{3\pm x}Ga_{3\pm x}$	YCd_6	14.5335(4)	–	–	3069.85(15)
$TbAu_{3\pm x}Ga_{3\pm x}$	YCd_6	14.4749(3)	–	–	3032.83(12)
$DyAu_{3\pm x}Ga_{3\pm x}$	YCd_6	14.4597(2)	–	–	3023.31(8)
$HoAu_{3\pm x}Ga_{3\pm x}$	YCd_6	14.4430(3)	–	–	3012.80(10)
$ErAu_{3\pm x}Ga_{3\pm x}$	YCd_6	14.4362(2)	–	–	3008.58(8)
$TmAu_{3\pm x}Ga_{3\pm x}$	YCd_6	14.3625(3)	–	–	2962.71(9)
$Er_{14}Au_{34+x}Ga_{17-x}$	$Gd_{14}Ag_{51}$	12.3680(3)	–	9.0397(3)	1197.51(5)
$Tm_{14}Au_{34+x}Ga_{17-x}$	$Gd_{14}Ag_{51}$	12.3122(5)	–	9.0514(5)	1188.28(10)
$GdAu_{1+x}Ga_{2-x}$	$MgCuAl_2$	4.49590(16)	10.3190(3)	6.6612(2)	309.034(18)
$TbAu_{1+x}Ga_{2-x}$	$MgCuAl_2$	4.47146(13)	10.2796(3)	6.65675(18)	305.977(14)
$DyAu_{1+x}Ga_{2-x}$	$MgCuAl_2$	4.45323(15)	10.2488(3)	6.6526(2)	303.628(17)
$HoAu_{1+x}Ga_{2-x}$	$MgCuAl_2$	4.43602(14)	10.2256(3)	6.6644(2)	302.304(16)
$ErAu_{1+x}Ga_{2-x}$	$MgCuAl_2$	4.42331(18)	10.1965(3)	6.6377(2)	299.376(19)
$TmAu_{1+x}Ga_{2-x}$	$MgCuAl_2$	4.40307(12)	10.1720(2)	6.65910(16)	298.247(13)
$GdAu_{1+x}Ga_{3-x}$	$BaAl_4$	4.17564(16)	–	11.0591(5)	192.826(13)
$Tb_3Au_{3+x}Ga_{8-x}$	La_3Al_{11}	4.24423(12)	9.9970(3)	12.4817(3)	529.59(2)
$Dy_3Au_{3+x}Ga_{8-x}$	La_3Al_{11}	4.23240(14)	9.9836(3)	12.4392(4)	525.61(3)
$Ho_3Au_{3+x}Ga_{8-x}$	La_3Al_{11}	4.22263(12)	9.9711(3)	12.4114(4)	522.57(3)
$Er_3Au_{3+x}Ga_{8-x}$	La_3Al_{11}	4.21031(15)	9.9590(4)	12.3712(5)	518.73(3)
$Tm_3Au_{3+x}Ga_{8-x}$	La_3Al_{11}	4.20241(13)	9.9399(3)	12.3608(4)	516.33(3)

Table 2 Atomic and thermal parameters in the structure of the Tm–Au–Ga compounds.

Atom	Site	*x*	*y*	*z*	B_{iso} (Å^2)	Occupation G
$TmAu_3Ga_7$						
Tm	6*b*	0	0	0	1.46(7)	1Tm
Au	18*e*	0.31971(16)	0	¼	1.00(3)	1Au
Ga1	6*a*	0	0	¼	1.27(17)	1Ga
Ga2	36*f*	0.0116(4)	0.2079(3)	0.13495(15)	0.71(6)	1Ga
Refinement composition: $TmAu_3Ga_7$. Reliability factors: R_B = 7.57 %, R_F = 5.14 %.						
$TmAu_{3\pm x}Ga_{3\pm x}$						
Tm	24*g*	0	0.1852(3)	0.3018(3)	1.00(9)	1Tm
*M*1	12*d*	0.4123(16)	0	0	1.25(6)	1Ga
*M*2	12*e*	0.2013(9)	0	½	1.25(6)	0.033(13)Au+0.967(13)Ga
*M*3	16*f*	0.1552(3)	0.1552(3)	0.1552(3)	1.25(6)	0.459(19)Au+0.541(19)Ga
*M*4	24*g*	0	0.3995(3)	0.3512(3)	1.25(6)	0.960(12)Au+0.040(12)Ga
*M*5	24*g*	0	0.2497(5)	0.0930(4)	1.25(6)	0.539(11)Au+0.461(11)Ga
*M*6	24*g*	0	0.0573(16)	0.0945(15)	1.25(6)	0.097(10)Au+0.236(10)Ga
*M*7	48*h*	0.1206(3)	0.3372(3)	0.2041(4)	1.25(6)	0.455(9)Au+0.546(9)Ga
Refinement composition: $TmAu_{2.83}Ga_{3.17}$. Reliability factors: R_B = 7.42 %, R_F = 7.05 %.						
$Tm_{14}Au_{34+x}Ga_{17-x}$						
Tm1	2*e*	0	0	0.3016(15)	0.57(11)	1Tm
Tm2	6*j*	0.1173(7)	0.3909(7)	0	0.57(11)	1Tm
Tm3	6*k*	0.4685(8)	0.1300(8)	½	0.57(11)	1Tm
*M*1	2*c*	⅓	⅔	0	1.18(8)	1Au
*M*2	4*h*	⅓	⅔	0.2878(16)	1.18(8)	0.18(2)Au+0.82(2)Ga
*M*3	6*j*	0.0393(20)	0.1386(15)	0	1.18(8)	0.279(18)Au+0.221(18)Ga
*M*4	6*k*	0.0596(8)	0.2342(7)	½	1.18(8)	0.58(2)Au+0.42(2)Ga
*M*5	12*l*	0.4892(6)	0.1093(5)	0.1476(8)	1.18(8)	0.458(12)Au+0.542(12)Ga
*M*6	12*l*	0.2713(5)	0.0712(5)	0.2289(7)	1.18(8)	0.752(14)Au+0.248(14)Ga
*M*7	12*l*	0.1178(4)	0.4474(4)	0.3362(5)	1.18(8)	1Au
Refinement composition: $Tm_{14}Au_{34.4}Ga_{16.6}$. Reliability factors: R_B = 6.86 %, R_F = 4.96 %.						
$TmAu_{1+x}Ga_{2-x}$						
Tm	4*c*	0	0.4132(2)	1/4	0.90(9)	1Tm
*M*1	4*c*	0	0.70517(19)	1/4	1.07(8)	0.856(12)Au+0.144(12)Ga
*M*2	8*f*	0	0.1196(2)	0.0532(4)	0.98(12)	0.209(10)Au+0.791(10)Ga
Refinement composition: $TmAu_{1.27}Ga_{1.73}$. Reliability factors: R_B = 6.91 %, R_F = 4.88 %.						
$Tm_3Au_{3+x}Ga_{8-x}$						
Tm1	2*a*	0	0	0	1.07(14)	1Tm
Tm2	4*i*	0	0	0.3133(3)	0.49(10)	1Tm
*M*1	2*d*	½	0	½	0.87(23)	0.045(9)Au+0.955(9)Ga
*M*2	4*h*	0	0.2114(4)	½	1.16(10)	0.514(7)Au+0.486(7)Ga
*M*3	8*l*	0	0.2798(5)	0.1446(4)	1.40(13)	0.031(5)Au+0.969(5)Ga
*M*4	8*l*	0	0.3693(2)	0.3391(3)	1.11(9)	0.472(8)Au+0.528(8)Ga
Refinement composition: $Tm_3Au_{3.09}Ga_{7.91}$. Reliability factors: R_B = 7.04 %, R_F = 5.97 %.						

the [Au_6] octahedra linked by common faces are occupied by the Ga tetrahedra; the remaining octahedral voids are filled by the rare-earth atoms.

The crystal chemical features of the gallides described above are similar to the earlier discovered RAu_3Al_7 compounds. Detailed information about synthesis and structure of these aluminides can be found in [10,32].

RAu$_{3\pm x}$*Ga*$_{3\pm x}$ *phases*

The $RAu_{3\pm x}Ga_{3\pm x}$ phases were found to adopt the structure type YCd_6 (space group *Im*-3, *Z* = 24, *cI*68). The rare-earth atoms occupy one independent position (Y, 24*g*). Seven independent positions (Cd, 12*d*, 12*e*, 16*f*, 24*g*, 24*g*, 24*g* and 48*h*) are filled by the gold and

Table 3 Crystal data and details of the refinement for the $GdAu_{1+x}Ga_{3-x}$, $Dy_3Au_{3+x}Ga_{8-x}$, and $Er_3Au_{3+x}Ga_{8-x}$ phases.

Empirical formula	$GdAu_{1.15}Ga_{2.85}$	$Dy_3Au_{2.81}Ga_{8.19}$	$Er_3Au_{2.57}Ga_{8.43}$
Relative mass	582.21	1611.73	1595.98
Crystal system	Tetragonal	Orthorhombic	Orthorhombic
Space group	*I*4/*mmm*	*Immm*	*Immm*
Pearson symbol	*tI*10	*oI*28	*oI*28
Unit cell dimensions			
a	4.1640(6) Å	4.2254(10) Å	4.2059(18) Å
b	4.1640(6) Å	9.961(4) Å	9.925(4) Å
c	11.029(3) Å	12.424(3) Å	12.358(5) Å
V	191.23(7) Å^3	522.9(3) Å^3	515.8(4) Å^3
Formula units per cell	2	2	2
Calculated density	10.111 g/cm^3	10.236 g/cm^3	10.275 g/cm^3
Crystal shape and color	Block, Silvery	Block, Silvery	Block, Silvery
Diffractometer	CAD4	CAD4	CAD4
Radiation	Mo K_α (λ=0.71073 Å)	Mo K_α (λ=0.71073 Å)	Mo K_α (λ=0.71073 Å)
Monochromator	Graphite	Graphite	Graphite
Temperature	293(2) K	293(2) K	293(2) K
Absorption coefficient	80.559 mm^{-1}	80.990 mm^{-1}	82.041 mm^{-1}
F(000)	486	1348	1337
θ range for data collection	3.69º to 34.99º	2.62º to 34.98º	2.63º to 34.98º
Scan type	ω-2θ	ω-2θ	ω-2θ
Range in *hkl*	±6, ±6, ±17	±6, ±12, ±18	±6, ±12, ±19
Total no. reflections	1621	3999	3651
Independent reflection	147	622	621
Reflections with $I > 2\sigma(I)$	119	514	392
Structure refinement	SHELXL-97	SHELXL-97	SHELXL-97
Refinement method	Full-matrix least-squares on F^2	Full-matrix least-squares on F^2	Full-matrix least-squares on F^2
Data/restraints/parameters	147/2/13	622/2/32	621/2/32
Goodness-of-fit on F^2	0.850	0.934	0.934
Final R indices [a]	R1=0.0435, *w*R2=0.1089	R1=0.0537, *w*R2=0.1025	R1=0.0641, *w*R2=0.1355
Weighting scheme [b]	*a*=0.0875, *b*=0	*a*=0.0385, *b*=0	*a*=0.0614, *b*=0
Extinction coefficient	0.0043(17)	0.0077(5)	0.0155(13)

[a] $R1=\sum(||F_o|-|F_c||)/\sum|F_o|$, $wR2=\{\sum w[(F_o^2-F_c^2)^2]/\sum w[(F_o^2)^2]\}^{1/2}$;
[b] $w=1/[\sigma^2(F_o^2)+(aP)^2+bP]$, in which $P=(F_o^2+2F_c^2)/3$].

Table 4 Atom coordinates and displacement parameters for $GdAu_{1.15}Ga_{2.85}$.

Atom coordinates and isotropic displacement parameters (Å^2)

Atom	Site	*x*	*y*	*z*	U_{eq}
Gd	2*a*	0	0	0	0.0104(6)
*M*1	4*d*	0	½	¼	0.0086(8)
*M*2	4*e*	0	0	0.38792(14)	0.0116(5)

*M*1 = 0.069(13)Au + 0.931(13)Ga, *M*2 = 0.505(13)Au + 0.495(13)Ga.

Anisotropic displacement parameters (Å^2)

Atom	U_{11}	U_{22}	U_{33}	U_{23}	U_{13}	U_{12}
Gd	0.0079(7)	0.0079(7)	0.0155(10)	0	0	0
*M*1	0.0093(10)	0.0093(10)	0.0071(13)	0	0	0
*M*2	0.0108(6)	0.0108(6)	0.0132(9)	0	0	0

*M*1 = 0.069(13)Au + 0.931(13)Ga, *M*2 = 0.505(13)Au + 0.495(13)Ga.

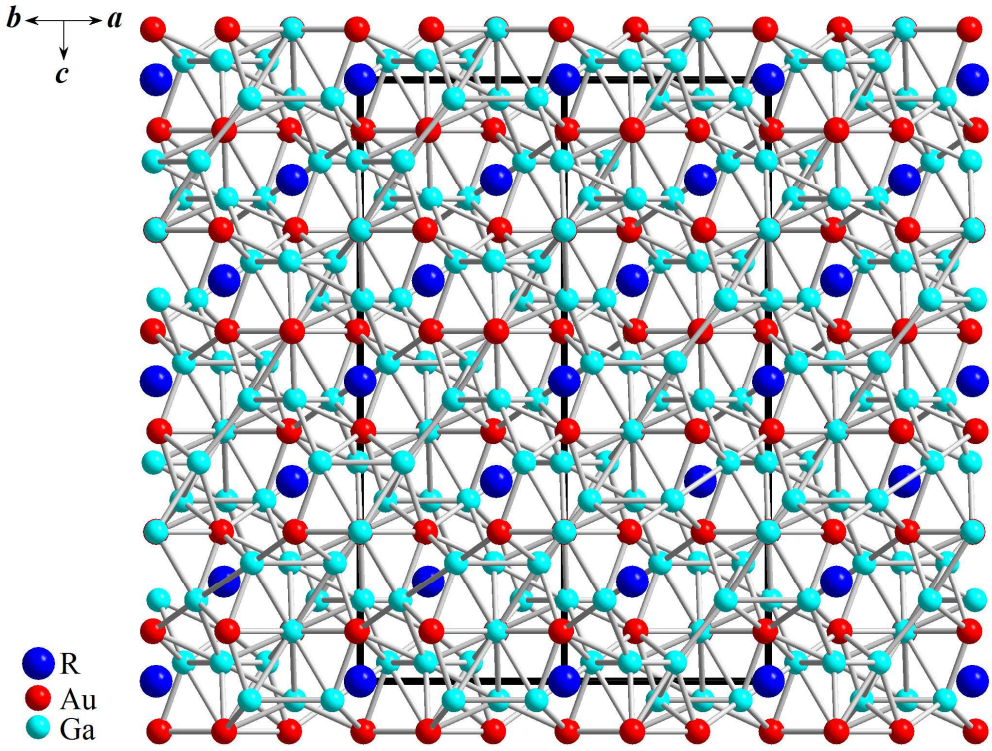

(*a*)

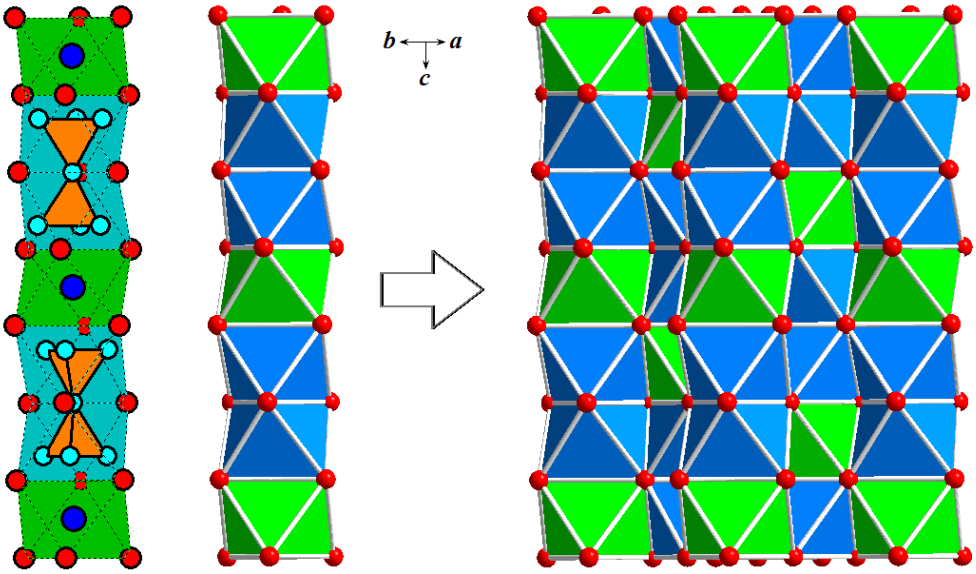

(*b*)

Fig. 2 View of the RAu_3Ga_7 structure approximately along the [110] direction. The unit cell, $[Au_3Ga_7]$ network (*a*) and condensed $[Au_6]$ octahedra (*b*) are emphasized. (Color figures are available in the electronic edition of the journal.)

gallium atoms, alone or as mixtures (*M*1-*M*7). The occupancy parameter of the *M*6 site was found to be equal to 33.3 %.

Fig. 3*a* shows the $RAu_{3\pm x}Ga_{3\pm x}$ structure as a complex three-dimensional $[Au_{3\pm x}Ga_{3\pm x}]$ network with rare-earth atoms (*R*) in voids (Fig. 3*a*). An analysis of the interatomic distances clearly indicated strong interactions between *R* and *M*, as well as between *M* atoms. The shortest interatomic distances were found to be 3.039-3.102 Å (*R*–*M*7), 3.069-3.112 Å (*R*–*M*5),

Table 5 Atom coordinates and displacement parameters for $Dy_3Au_{2.81}Ga_{8.19}$.

Atom coordinates and isotropic displacement parameters (Å^2)

Atom	Site	*x*	*y*	*z*	U_{eq}
Dy1	2*a*	0	0	0	0.0079(5)
Dy2	4*i*	0	0	0.31727(11)	0.0063(4)
*M*1	2*d*	½	0	½	0.0126(11)
*M*2	4*h*	0	0.2145(2)	½	0.0118(6)
*M*3	8*l*	0	0.2738(3)	0.1443(2)	0.0142(6)
*M*4	8*l*	0	0.36677(17)	0.33767(11)	0.0146(5)

*M*1 = 1Ga, *M*2 = 0.506(14)Au + 0.494(14)Ga, *M*3 = 1Ga, *M*4 = 0.449(12)Au + 0.551(12)Ga.

Anisotropic displacement parameters (Å^2)

Atom	U_{11}	U_{22}	U_{33}	U_{23}	U_{13}	U_{12}
Dy1	0.0087(9)	0.0104(10)	0.0047(9)	0	0	0
Dy2	0.0068(7)	0.0084(7)	0.0036(6)	0	0	0
*M*1	0.021(3)	0.014(3)	0.003(2)	0	0	0
*M*2	0.0144(10)	0.0159(11)	0.0050(8)	0	0	0
*M*3	0.0135(12)	0.0140(13)	0.0150(13)	–0.0038(10)	0	0
*M*4	0.0101(7)	0.0240(9)	0.0096(8)	0.0034(5)	0	0

*M*1 = 1Ga, *M*2 = 0.506(14)Au + 0.494(14)Ga, *M*3 = 1Ga, *M*4 = 0.449(12)Au + 0.551(12)Ga.

Table 6 Atom coordinates and isotropic displacement parameters for $Er_3Au_{2.57}Ga_{8.43}$.

Atom coordinates and isotropic displacement parameters (Å^2)

Atom	Site	*x*	*y*	*z*	U_{eq}
Er1	2*a*	0	0	0	0.0047(5)
Er2	4*i*	0	0	0.31719(13)	0.0061(5)
*M*1	2*d*	½	0	½	0.0112(13)
*M*2	4*h*	0	0.2119(3)	½	0.0112(6)
*M*3	8*l*	0	0.2744(4)	0.1451(3)	0.0115(8)
*M*4	8*l*	0	0.3679(2)	0.33887(13)	0.0122(6)

*M*1 = 1Ga, *M*2 = 0.430(16)Au + 0.570(16)Ga, *M*3 = 1Ga, M4 = 0.428(13)Au + 0.572(13)Ga.

Anisotropic displacement parameters (Å^2)

Atom	U_{11}	U_{22}	U_{33}	U_{23}	U_{13}	U_{12}
Er1	0.0000(8)	0.0128(12)	0.0013(9)	0	0	0
Er2	0.0000(6)	0.0140(10)	0.0043(7)	0	0	0
*M*1	0.004(2)	0.026(4)	0.004(2)	0	0	0
*M*2	0.0090(10)	0.0182(14)	0.0065(10)	0	0	0
*M*3	0.0064(12)	0.0167(19)	0.0114(15)	–0.0022(12)	0	0
*M*4	0.0051(8)	0.0255(13)	0.0061(9)	0.0033(6)	0	0

*M*1 = 1Ga, *M*2 = 0.430(16)Au + 0.570(16)Ga, *M*3 = 1Ga, M4 = 0.428(13)Au + 0.572(13)Ga.

3.096-3.138 Å (*R*–*M*3) 3.035-3.156 Å (*R*–*M*1), 2.293-2.746 Å (*M*1–*M*1), 2.690-2.853 Å (*M*1–*M*5), 2.581-2.600 Å (*M*2–*M*4), 2.735-2.810 Å (*M*3–*M*6), 2.758-2.785 Å (*M*3–*M*5), 2.710-2.802 Å (*M*3–*M*7), 2.782-2.801 Å (*M*4–*M*7), 2.632-2.726 Å (*M*5–*M*6), 2.664-2.736 Å (*M*5–*M*7), 2.636-2.753 Å (*M*5–*M*5), and 2.657-2.762 Å (*M*7–*M*7).

The structure of the $RAu_{3\pm x}Ga_{3\pm x}$ phases can also be described as a body-centered-cubic arrangement of tricontahedral cluster units (Fig. 3*b*). Each of these encapsulated clusters is made up of five endohedral shells (Fig. 3*c*), from the center out: a disordered tetrahedron [*M*6], a pentagonal dodecahedron [$M3_8M5_{12}$], an icosahedron [R_{12}], an icosidodecahedron [$M1_6M7_{24}$], and a triacontahedron [$M2_{24}M4_{36}M7_{24}$]. The coordination polyhedra of the *R* atoms can be considered as full-capped deformed pentagonal prisms. The *M*1 and *M*7 atoms are surrounded by tri-capped and four-capped deformed trigonal prisms, respectively. The *M*2, *M*3, *M*4, and *M*5 atoms are situated at the centers of defect or deformed icosahedra. The coordination environments of the *M*6 atoms are non-coplanar pentagons or pentagonal pyramids.

It should be noted that intermetallic phases with YCd_6-type and related structures have been found to exist in many ternary systems. Detailed descriptions of some gold-containing structures are given in [33-38].

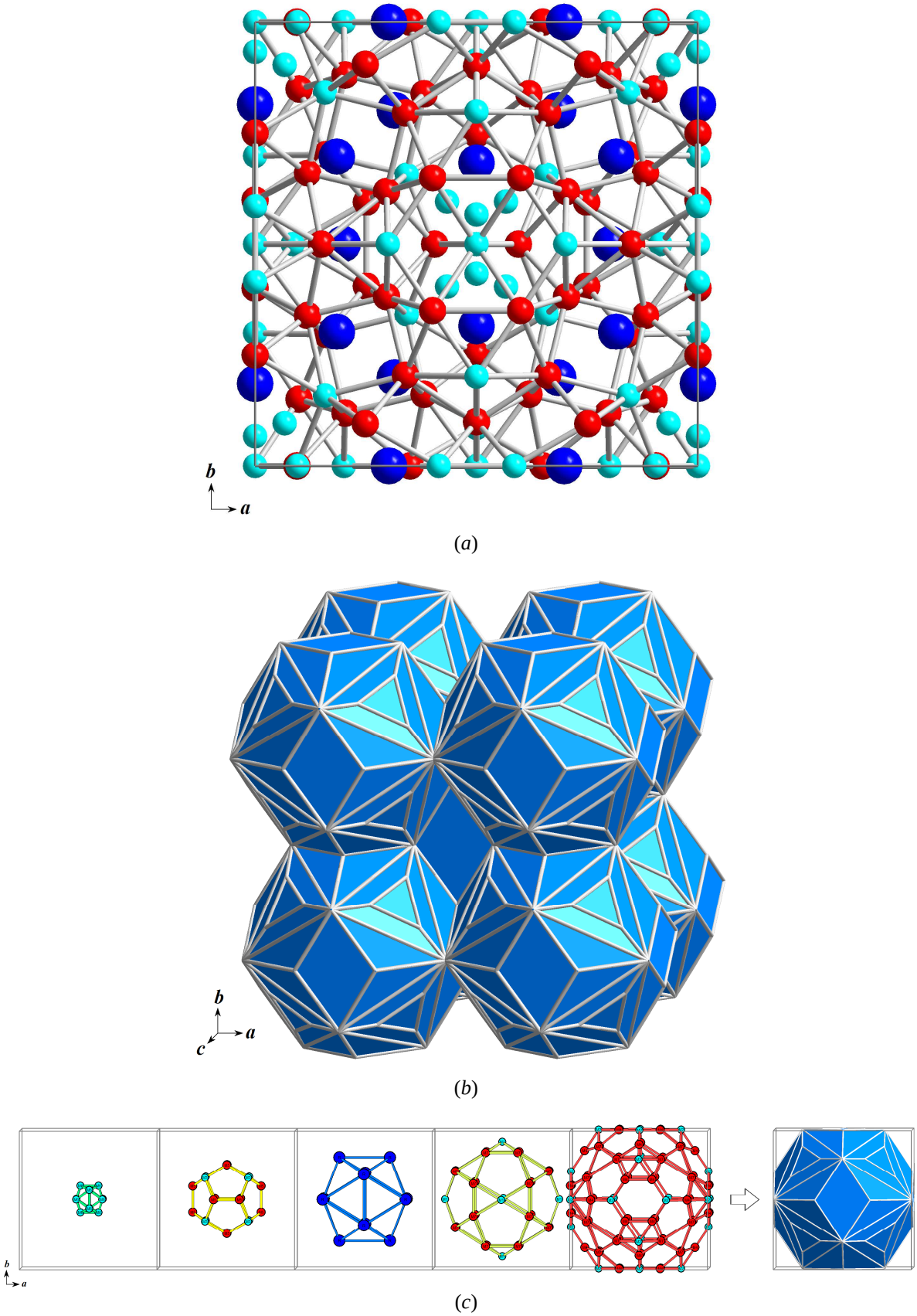

Fig. 3 Projection of the unit cell of $RAu_{3\pm x}Ga_{3\pm x}$ onto the *ab* plane emphasizing the $[Au_3Ga_3]$ network (*a*) (the *M*6–*M*6 connections are not shown). A bcc packing of tricontahedral cluster units (*b*). Endohedral atomic shells within the tricontahedral cluster (*c*). Rare-earth, gold, gallium and mixed Au/Ga atoms are drawn as blue, red and cyan spheres.

$R_{14}Au_{34+x}Ga_{17-x}$ phases

Ternary $R_{14}Au_{34+x}Ga_{17-x}$ (*R* = Er and Tm) phases with $Gd_{14}Ag_{51}$ structure type (space group *P*6/*m*, *Z* = 1, *hP*65) were found (Fig. 4*a*). The atoms of this type are positioned at the ten sites. The Er or Tm (*R*1-*R*3) atoms occupy the Gd sites (2*e*, 6*j*, and 6*k*), while the Au and Ga atoms (*M*1-*M*7) are situated in the Ag sites (2*c*, 4*h*, 6*j*, 6*k*, 12*l*, 12*l*, and 12*l*).

The structure of the $R_{14}Au_{34+x}Ga_{17-x}$ phases can be shown as a packing of two different types of layer (slab) along the *Z* direction (Fig. 4*b*). These layers are the aggregation of six-membered "wheels", which are composed by the coordination polyhedra of the *R*2 and *R*3 atoms (Fig. 4*c*). The hexagonal cavities, which are located at the centers of these wheels, are filled by the *R*1 atoms (Fig. 4*c*).

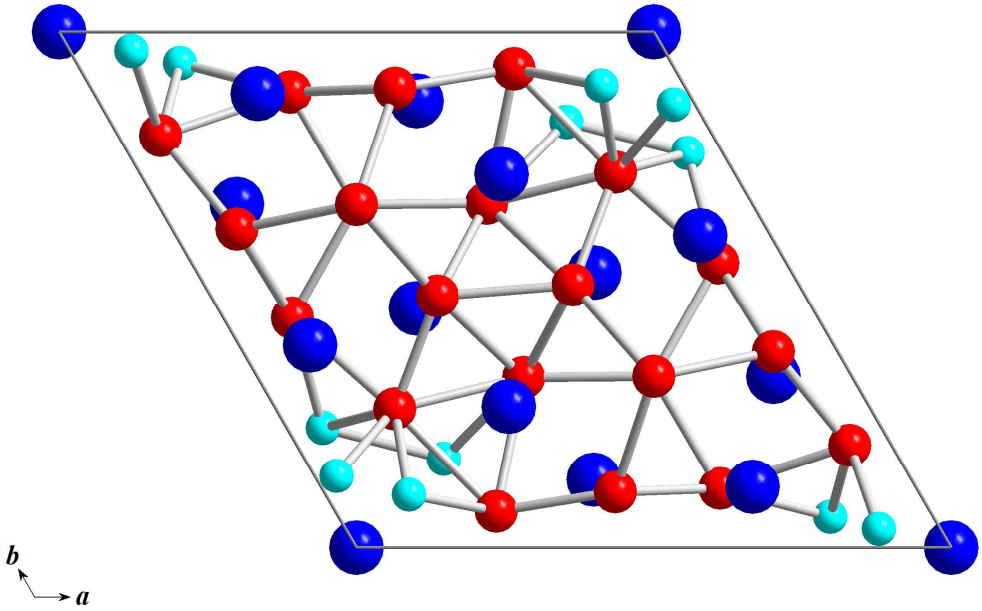

(*a*)

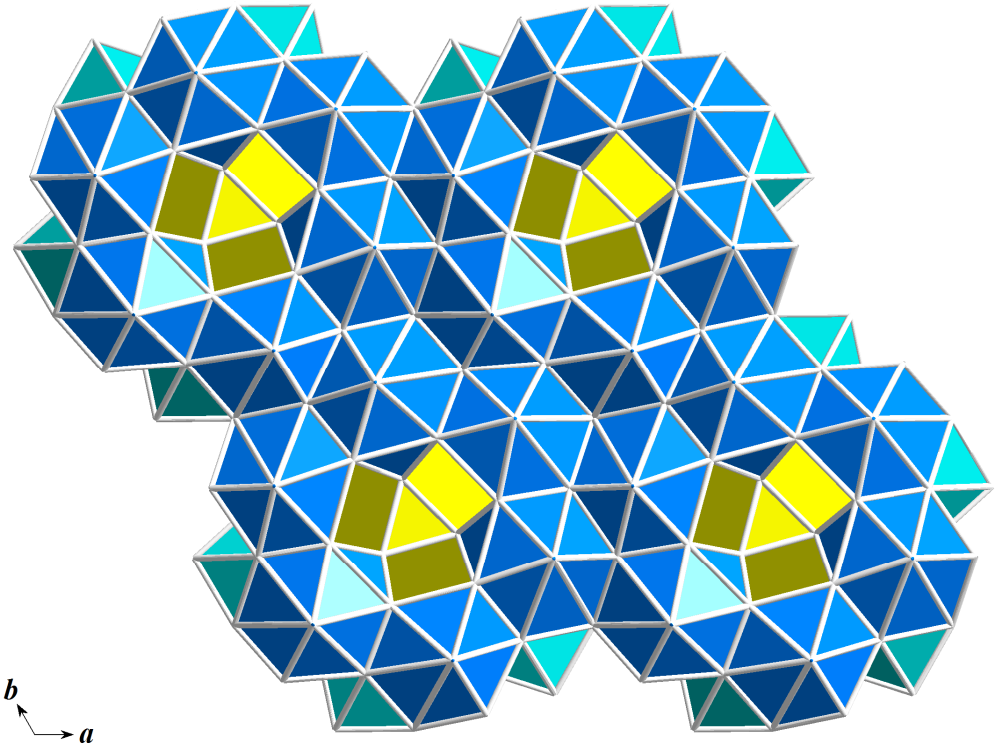

(*b*)

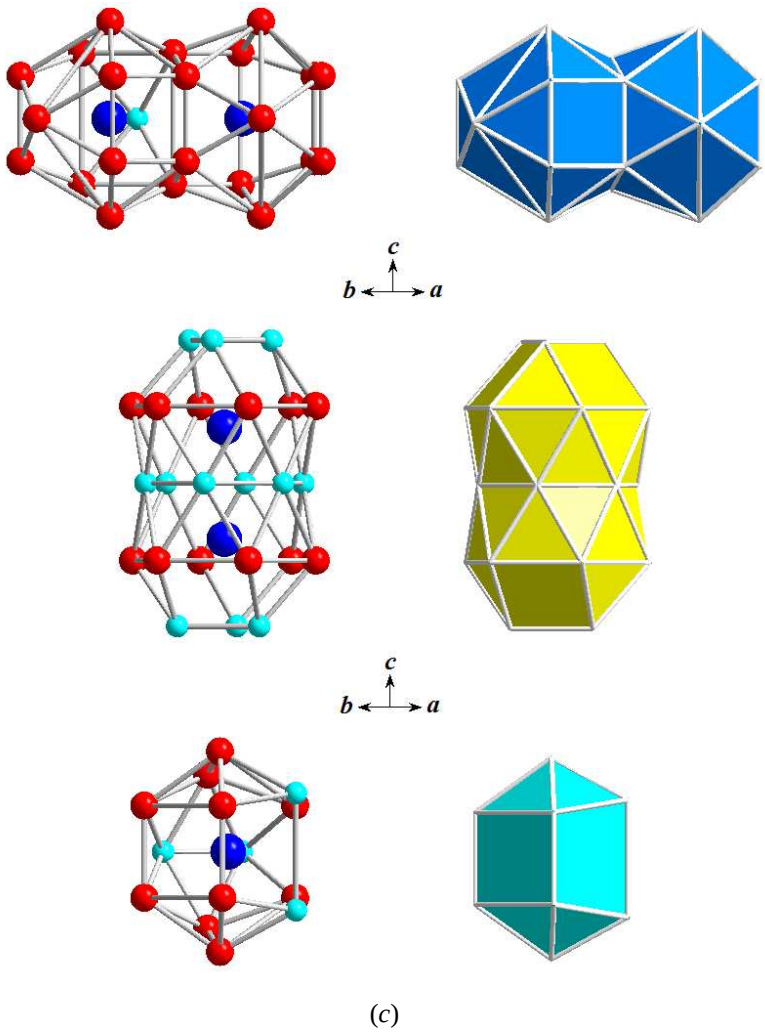

(*c*)

Fig. 4 The $R_{14}Au_{34+x}Ga_{17-x}$ structure (*a*). The network of condensed polyhedra of the rare-earth atoms (*b*). The near-neighbor coordination of the *R*1 (yellow sphere), *R*2 (blue sphere) and *R*3 (cyan sphere) atoms (*c*). Rare-earth, gold, gallium and mixed Au/Ga atoms are shown by blue, red and cyan balls.

The shortest interatomic distances in the $R_{14}Au_{34+x}Ga_{17-x}$ structures occur between *R* and *M* and between *M* atoms, covering wide ranges. Many of them were found to be shorter than the sums of the atomic radii of the respective components [31], indicating significant *R*–*M* and *M*–*M* interactions: 3.071-3.079 Å (*R*1–*M*6), 3.094-3.082 Å (*R*2–*M*1), 2.755-2.771 Å (*R*2–*M*3), 3.035-3.051 Å (*R*2–*M*5), 3.000-3.025 Å (*R*2–*M*6), 3.121-3.137 Å (*R*2–*M*7), 3.101-3.131 Å (*R*3–*M*2), 2.961-3.035 Å (*R*3–*M*7), 2.605-2.668 Å (*M*1–*M*2), 2.713-2.736 Å (*M*2–*M*7), 2.638-2.693 Å (*M*3–*M*3), 2.757-2.783 Å (*M*3–*M*6), 2.596 Å (*M*4–*M*4), 2.779-2.782 Å (*M*4–*M*7), 2.672-2.701 Å (*M*5–*M*5), 2.589-2.611 Å (*M*5–*M*6) and 2.769-2.771 Å (*M*5–*M*7). Distorted 16-, 14- and 15-vertex Frank-Kasper polyhedra are centered by the *R*1, *R*2 and *R*3 atoms, respectively. The *M*1 atoms are located inside fully capped trigonal prisms. Four-capped and tri-capped distorted trigonal prisms are polyhedra for the *M*2 and *M*3 atoms. The *M*4 and *M*6 atoms are coordinated by deformed icosahedra, while the *M*5 and *M*6 atoms are surrounded by defected icosahedra.

Among the investigated gallium based ternary systems, intermediate phases with $Gd_{14}Ag_{51}$ or related defect/filled types were identified in the {Sc, Y, Nd, Sm, Gd-Tm, Lu, U}–Cu–Ga [39-41] and Yb–{Ag, Au}–Ga [11] systems. The formation of solid solutions, with extended homogeneity ranges, based on binary compounds with $Gd_{14}Ag_{51}$ structure type is also common in many rare-earth – *d*-metal – gallium systems [5,42].

RAu$_{1+x}$Ga$_{2-x}$ phases

The crystal structure of the *R*Au$_{1+x}$Ga$_{2-x}$ phases represents a partially disordered version of the MgCuAl$_2$ structure type (space group *Cmcm*, *Z* = 4, *oS*16). The rare-earth (*R*) atoms occupy the magnesium (4*c*) sites, while statistical gold-rich (*M*1) and gallium-rich (*M*2) mixtures occupy the copper (4*c*) and aluminum (8*f*) positions, respectively. The *M*2 atoms build up three-dimensional networks, where strongly puckered, elongated hexagons along the *Y* direction can be seen (left part of Fig. 5). The shortest *M*2–*M*2 distances within and between these hexagons range from 2.493 to 2.552 Å and from 2.621 to 2.659 Å, respectively. These *M*2–*M*2 distances compare well with those (2.78 Å) in pure gallium metal. Together, the *M*1 and *M*2 atoms form a three-dimensional [Au$_{1+x}$Ga$_{2-x}$] network with pentagonal-prismatic channels along the *X* direction (central part of Fig. 5). Rare-earth atoms are located inside these channels. The *M*1–*M*2 (2.693-2.729 Å and 2.706-2.745 Å) distances within the [Au$_{1+x}$Ga$_{2-x}$] network are shorter than the sum of the metallic radii (2.83 Å Au + Ga) [31], indicative of substantial *M*1–*M*2 bonding. Strong interactions are also observed between *R* and *M*1 and *M*2 atoms. The shortest interatomic distances were found to be 2.970-3.100 Å (*R*–*M*1) and 2.989-3.033 Å (*R*–*M*2). An alternative description of the *R*Au$_{1+x}$Ga$_{2-x}$ structure as a packing of the coordination polyhedra of the *R* atoms is shown in the right part of Fig. 5. Here, the coordination spheres (equatorially capped pentagonal prisms) of the rare-earth atoms consist of thirteen neighboring atoms (three *M*1 and ten *M*2 atoms) and are condensed by common faces. From a purely geometrical point of view, the *M*1 and *M*2 atoms in the *R*Au$_{1+x}$Ga$_{2-x}$ structure have coordination polyhedra in form of equatorially tri-capped and four-capped trigonal prisms, respectively.

Intermetallic compounds *RMX*$_2$ (*R* = rare-earth, *M* = *d*- and *X* = *p*-metal) with MgCuAl$_2$ structure type are known for many aluminum-, gallium-, indium- and tin-containing ternary systems [9,42]. Structural studies of them have been performed mainly for the stoichiometric composition 1:1:2, while the homogeneity ranges have been investigated only for the YbNi$_{1+x}$Ga$_{2-x}$ and LuAu$_{1+x}$Ga$_{2-x}$ phases [25,43]. Defect representatives of the MgCuAl$_2$ structure type, *e.g.* CeRu$_{0.88}$In$_2$ and Yb$_{0.95}$PtIn$_2$, are also described in the literature [44,45].

R$_3$Au$_{3+x}$Ga$_{8-x}$ phases

Several ternary *R*$_3$Au$_{3+x}$Ga$_{8-x}$ phases crystallize with the structure type La$_3$Al$_{11}$ (space group *Immm*, *Z* = 2, *oI*26) (Fig. 6*a*). Two crystallographically independent rare-earth sites (*R*1, 2*a* and *R*2, 4*i*) build a body-centered tetragonal sublattice, while the *M*1-*M*4 (Au and Ga) atoms form a three-dimensional polyanionic networks (Fig. 6*b*). Sites *M*1 (2*d*) and *M*3 (8*l*) are occupied mainly by Ga atoms. The *M*2 (4*h*) and *M*4 (8*l*) positions display an occupation by Au and Ga atoms close to the 1:1 ratio. The *R*1 and *R*2 atoms are coordinated by 20 and 19 atoms forming pseudo

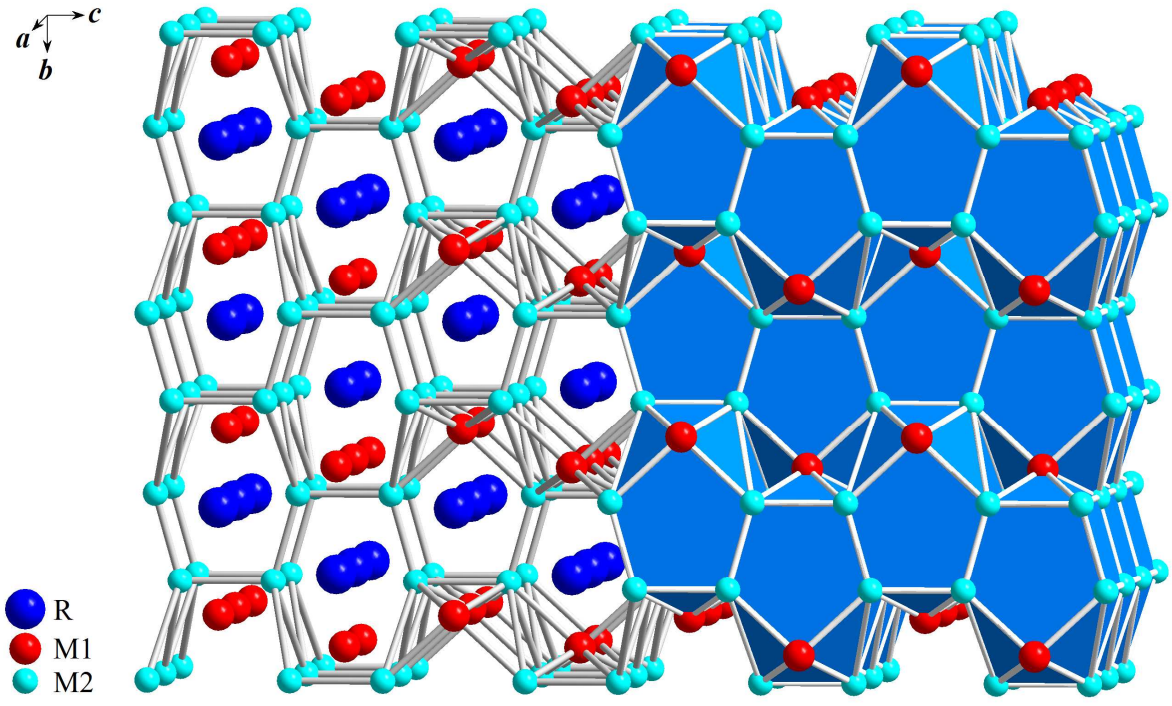

Fig. 5 The crystal structure of the *R*Au$_{1+x}$Ga$_{2-x}$ along the *X* axis. The three-dimensional [Au$_{1+x}$Ga$_{2-x}$] networks are outlined.

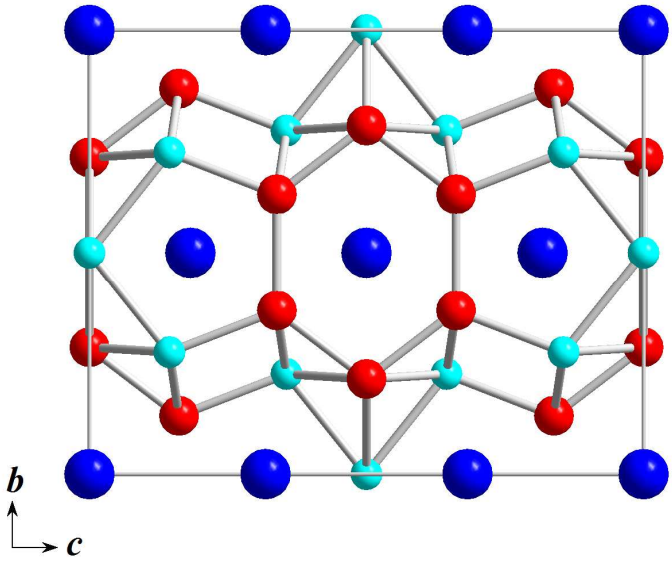

(*a*)

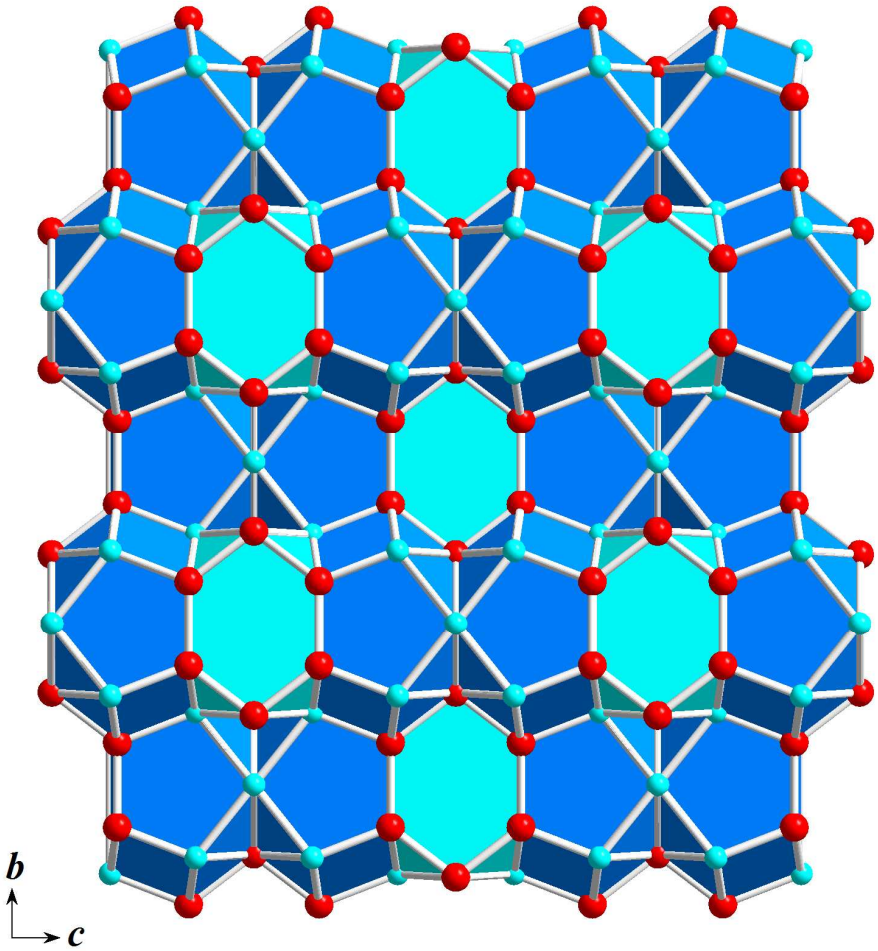

(*b*)

Fig. 6 Unit cell content (*a*) and three-dimensional network in the structure of the $R_3Au_{2+x}Ga_{9-x}$ phases. Blue, red and cyan balls indicate rare-earth, gold, gallium and mixed Au/Ga atoms.

Frank-Kasper polyhedra. The shortest *R*–*M* distances are lower than the sums of the atomic radii for the following atoms: 3.101-3.121 Å (*R*2–*M*1), 3.105-3.139 Å (*R*2–*M*2), 3.078-3.139 Å (*R*2–*M*3), and 3.107-3.166 Å (*R*2–*M*4). The coordination polyhedra around the *M*1 and *M*2 atoms can be described as distorted cubooctahedra. The *M*3 atoms are located inside monocapped distorted cubooctahedra. Tri-capped deformed trigonal prisms are the coordination polyhedra for the *M*4 atoms. The *M*–*M* distances cover a wide range, however, significant interactions were found between the following neighbors: 2.517-2.541 Å (*M*2–*M*4), 2.747-2.787 Å (*M*2–*M*3), 2.552-2.610 Å (*M*3–*M*4), 2.598-2.659 Å (*M*4–*M*4).

It should be underlined that the atomic arrangement of the La_3Al_{11} structure type is assigned to a large group of ternary intermetallic compounds [42], which are described as disordered or partially ordered phases. Representatives with different degrees of distortion of the La_3Al_{11} structure, such as $Yb_3Au_{5.5}Ga_{5.5}$, $Ca_3Au_{7.16}Ge_{3.84}$, $Ca_3Au_8Ge_3$, $La_3Au_4In_7$, and $Er_3Pd_7P_4$, are also known [42].

References

[1] E.I. Gladyshevskiy, *Crystal Chemistry of Silicides and Germanides*, Metallurgiya, Moscow, 1971 (in Russian).

[2] E.I. Gladyshevskiy, O.I. Bodak, *Crystal Chemistry of Rare-earth Based Intermetallic Compounds*, Vyshcha Shkola, Lviv, 1982 (in Russian).

[3] Yu.B. Kuzma, *Crystal Chemistry of Borides*, Vyshcha Shkola, Lviv, 1983 (in Russian).

[4] O.I. Bodak, E.I. Gladyshevskiy, *Ternary Systems Containing Rare-earth Metals*, Vyshcha Shkola, Lviv, 1985 (in Russian).

[5] Yu.N. Grin, R.E. Gladyshevskiy, *Gallides*, Metallurgiya, Moscow, 1989 (in Russian).

[6] Yu.B. Kuzma, N. Chaban, *Binary and Ternary Systems Containing Boron*, Metallurgiya, Moscow, 1990 (in Russian).

[7] R.V. Skolozdra, *Stannides of Transition and Rare-earth Elements*, Svit, Lviv, 1993 (in Ukranian).

[8] K.A. Gschneidner, J.-C. Bünzli, V.K. Pecharsky, *Handbook on the Physics and Chemistry of Rare Earths*, Elsevier, Amsterdam, Vols. 1-43, 1978-2013.

[9] P. Villars (Ed.), *Pearson's Handbook, Crystallographic Data for Intermetallic Phases*, Desk Ed., ASM, Materials Park, OH, 1997.

[10] Yu. Verbovytskyy, *Chem. Met. Alloys* 5 (2012) 23-32.

[11] R.V. Gumeniuk, *Ph.D. Thesis*, Ivan Franko National University of Lviv, Ukraine, 2003 (in Ukranian).

[12] Yu.N. Grin, M. Ellner, K. Hiebl, P. Rogl, *J. Alloys Compd.* 196 (1993) 207-212.

[13] Yu.N. Grin, M. Ellner, B. Predel, K. Peters, *J. Alloys Compd.* 201 (1993) 209-215.

[14] Yu.N. Grin, M. Ellner, K. Hiebl, P. Rogl, O.M. Sichevich, O.M. Myakush, *J. Alloys Compd.* 205 (1994) 285-289.

[15] Yu.N. Grin, M. Ellner, B. Predel, B. Baumgartner, *J. Solid Sate Chem.* 114 (1995) 342-345.

[16] G. Cordier, Ch. Dietrich, *Z. Kristallogr.* 211 (1996) 118.

[17] D. Rossi, R. Ferro, *Intermetallics* 8 (2000) 877-880.

[18] D. Rossi, R. Ferro, *J. Alloys Compd.* 317-318 (2001) 521-524.

[19] R. Gumeniuk, E. Bischoff, U. Burkhardt, Yu. Prots, W. Schnelle, L. Vasylechko, M. Schmidt, Yu. Kuzma, Yu. Grin, *J. Solid Sate Chem.* 182 (2009) 3374-3382.

[20] A.E. Dwight, *J. Less-Common. Met.* 127 (1987) 175-178.

[21] Y.N. Grin, P. Rogl, K. Hiebl, F.E. Wagner, H. Noël, *J. Solid State Chem.* 70 (1987) 168-177.

[22] Y. Grin, O.M. Sichevich, O.R. Myakush, *Sov. Phys. Crystallogr.* 36 (1991) 503-505.

[23] F. Hulliger, *J. Alloys Compd.* 218 (1995) 255-258.

[24] H. Flandorfer, P. Rogl, E. Bauer, H. Michor, R.Hatzl, E. Gratz, C. Godar, *J. Phys.: Condens. Matter* 8 (1996) 2365-2376.

[25] Yu. Grin, B. Baumgartner, *Mater. Sci. Forum* 166-169 (1994) 473-478.

[26] G. Cordier, C. Dietrich, T. Friedrich, *Z. Kristallogr.* 211 (1996) 627-628.

[27] G. Nolze, W. Kraus, *Powder Cell for Windows* (Version 2.3), Federal Institute for Materials Research and Testing, Berlin, 1999.

[28] D. Schwarzenbach, *Program LATCON*, University of Lausanne, Switzerland, 1975.

[29] J. Rodriguez-Carvajal, T. Roisnel, *FullProf.98 and WinPLOTR: New Windows 95/NT Applications for Diffraction, Commission for Powder Diffraction, International Union for Crystallography, Newsletter* (20) (1998).

[30] G.M. Sheldrick, *SHELX-97, A Program System for the Solution and Refinement of Crystal Structures*, Universität Göttingen, Germany, 1997.

[31] G.B. Bokiy, *Crystal Chemistry*, 3rd Ed., Nauka, Moscow, 1971 (in Russian).

[32] S.E. Latturner, D. Bilc, J.R. Ireland, C.R. Kannewurf, S.D. Mahanti, M.G. Kanatzidis, *J. Solid State Chem.* 170 (2003) 48-57.

[33] Q. Lin, J.D. Corbett, *J. Am. Chem. Soc.* 129 (2007) 6789-6797.

[34] Q. Lin, J.D. Corbett, *Inorg. Chem.* 47 (2008) 7651-7659.

[35] Q. Lin, J.D. Corbett, *Inorg. Chem.* 49 (2010) 10436-10444.

[36] T. Ishimasa, Y. Tanaka, S. Kashimoto, *Philos. Mag.* 91 (2011) 4218-4229.
[37] G.H. Gebresenbut, R. Tamura, D. Eklöf, C.P. Gómez, *J. Phys.: Condens. Matter* 25 (2013) 135402 (11 p.).
[38] T. Hiroto, G.H. Gebresenbut, C.P. Gómez, Y. Muro, M. Isobe, Y. Ueda, K. Tokiwa, R. Tamura, *J. Phys.: Condens. Matter* 25 (2013) 426004 (6 p.).
[39] L.A. Bulavin, V.A. Makara, P.P. Kuzmenko, *Sci. Rep. Taras Shevchenko Univ. Kiev, Ukr.SSR*, 1990, pp. 23-103 (in Russian).
[40] O.B. Mykhalitchko, *Ph.D. Thesis*, Ivan Franko National University of Lviv, Ukraine, 2013 (in Ukranian).
[41] Yu. Verbovytskyy, A.P Gonçalves, *Intermetallics* 33 (2013) 16-26.
[42] P. Villars, K. Cenzual (Eds.), *Pearson's Crystal Data – Crystal Structure Database for Inorganic Compounds*, ASM International, Material Park, OH, Release 2010/2011.
[43] L. Vasylechko, U. Burkhardt, W. Schnelle, H. Borrmann, F. Haarmann, A. Senyshyn, D. Trots, K. Hiebl, Yu. Grin, *Solid State Sci.* 14 (2012) 746-760.
[44] E.V. Murashova, A.I. Tursina, Zh.M. Kurenbaeva, A.V. Gribanov, Yu.D. Seropegin, *J. Alloys Compd*. 454 (2008) 206-209.
[45] A.C. Malingowski, M. Kim, J. Liu, L. Wu, M.C. Aronson, P.G. Khalifah, *J. Solid State Chem*. 198 (2013) 308-315.